Supplementary Material: Designing 3D Anisotropic Frame Fields with Odeco Tensors

HAIKUAN ZHU, Wayne State University, USA
HONGBO LI, Wayne State University, USA
HSUEH-TI DEREK LIU, Roblox & University of British Columbia, Canada
WENPING WANG, Texas A&M University, USA
JING HUA, Wayne State University, USA
ZICHUN ZHONG*, Wayne State University, USA

CCS Concepts: • **Computing methodologies → Volumetric models**; **Shape analysis**; **Mesh geometry models**.

Additional Key Words and Phrases: 3D tensor field design, anisotropic odeco tensor, anisotropic meshing, microstructure

ACM Reference Format:
Haikuan Zhu, Hongbo Li, Hsueh-Ti Derek Liu, Wenping Wang, Jing Hua, and Zichun Zhong. 2025. Supplementary Material: Designing 3D Anisotropic Frame Fields with Odeco Tensors. *ACM Trans. Graph.* 44, 4, Article 0 (August 2025), 4 pages. https://doi.org/10.1145/3731181

1 THEORETICAL AUXILIARIES

1.1 Angular Momentum Operators and Rotation Matrices

Here we list the angular momentum operators $\boldsymbol{L}_x, \boldsymbol{L}_y, \boldsymbol{L}_z$ and corresponding rotation matrices:

$$
\begin{aligned}
\boldsymbol{L}_x &= Diag(0, \boldsymbol{L}_x^{(2)}, \boldsymbol{L}_x^{(4)}) \ \in \mathbb{R}^{15\times 15},\\
\boldsymbol{L}_y &= Diag(0, \boldsymbol{L}_y^{(2)}, \boldsymbol{L}_y^{(4)}) \ \in \mathbb{R}^{15\times 15},\\
\boldsymbol{L}_z &= Diag(0, \boldsymbol{L}_z^{(2)}, \boldsymbol{L}_z^{(4)}) \ \in \mathbb{R}^{15\times 15},\\
e^{\theta_i^z \boldsymbol{L}_z} &= Diag(1, \boldsymbol{R}_z^{(2)}(\theta_i^z), \boldsymbol{R}_z^{(4)}(\theta_i^z)) \ \in \mathbb{R}^{15\times 15},\\
e^{\theta_i^y \boldsymbol{L}_y} &= Diag(1, \boldsymbol{R}_y^{(2)}(\theta_i^y), \boldsymbol{R}_y^{(4)}(\theta_i^y)) \ \in \mathbb{R}^{15\times 15},\\
e^{\theta_i^x \boldsymbol{L}_x} &= Diag(1, \boldsymbol{R}_x^{(2)}(\theta_i^x), \boldsymbol{R}_x^{(4)}(\theta_i^x)) \ \in \mathbb{R}^{15\times 15},\\
\boldsymbol{R}_y(\theta_i^y) &= \boldsymbol{R}_x(\pi/2)\boldsymbol{R}_z(\theta_i^y)\boldsymbol{R}_x(\pi/2)^T,\\
\boldsymbol{R}_x(\theta_i^x) &= \boldsymbol{R}_y(\pi/2)^T\boldsymbol{R}_z(\theta_i^x)\boldsymbol{R}_y(\pi/2),
\end{aligned}
$$

$$
\boldsymbol{L}_x^{(2)} = \begin{bmatrix} 0 & 0 & 0 & -1 & 0\\ 0 & 0 & -\sqrt{3} & 0 & -1\\ 0 & \sqrt{3} & 0 & 0 & 0\\ 1 & 0 & 0 & 0 & 0\\ 0 & 1 & 0 & 0 & 0 \end{bmatrix}, \boldsymbol{L}_y^{(2)} = \begin{bmatrix} 0 & 1 & 0 & 0 & 0\\ -1 & 0 & 0 & 0 & 0\\ 0 & 0 & 0 & -\sqrt{3} & 0\\ 0 & 0 & \sqrt{3} & 0 & -1\\ 0 & 0 & 0 & 1 & 0 \end{bmatrix},
$$

$$
\boldsymbol{L}_z^{(2)} = \begin{bmatrix} 0 & 0 & 0 & 0 & 2\\ 0 & 0 & 0 & 1 & 0\\ 0 & 0 & 0 & 0 & 0\\ 0 & -1 & 0 & 0 & 0\\ -2 & 0 & 0 & 0 & 0 \end{bmatrix}, \boldsymbol{L}_z^{(4)} = \begin{bmatrix} 0 & 0 & 0 & 0 & 0 & 0 & 0 & 0 & 4\\ 0 & 0 & 0 & 0 & 0 & 0 & 0 & 3 & 0\\ 0 & 0 & 0 & 0 & 0 & 0 & 2 & 0 & 0\\ 0 & 0 & 0 & 0 & 0 & 1 & 0 & 0 & 0\\ 0 & 0 & 0 & 0 & 0 & 0 & 0 & 0 & 0\\ 0 & 0 & 0 & -1 & 0 & 0 & 0 & 0 & 0\\ 0 & 0 & -2 & 0 & 0 & 0 & 0 & 0 & 0\\ 0 & -3 & 0 & 0 & 0 & 0 & 0 & 0 & 0\\ -4 & 0 & 0 & 0 & 0 & 0 & 0 & 0 & 0 \end{bmatrix},
$$

$$
\boldsymbol{L}_x^{(4)} = \begin{bmatrix} 0 & 0 & 0 & 0 & 0 & 0 & 0 & -\sqrt{2} & 0\\ 0 & 0 & 0 & 0 & 0 & 0 & -\frac{\sqrt{7}}{2} & 0 & -\sqrt{2}\\ 0 & 0 & 0 & 0 & 0 & -\frac{3}{\sqrt{2}} & 0 & -\frac{\sqrt{7}}{2} & 0\\ 0 & 0 & 0 & 0 & -\sqrt{10} & 0 & -\frac{3}{\sqrt{2}} & 0 & 0\\ 0 & 0 & 0 & \sqrt{10} & 0 & 0 & 0 & 0 & 0\\ 0 & 0 & \frac{3}{\sqrt{2}} & 0 & 0 & 0 & 0 & 0 & 0\\ 0 & \frac{\sqrt{7}}{2} & 0 & \frac{3}{\sqrt{2}} & 0 & 0 & 0 & 0 & 0\\ \sqrt{2} & 0 & \frac{\sqrt{7}}{2} & 0 & 0 & 0 & 0 & 0 & 0\\ 0 & \sqrt{2} & 0 & 0 & 0 & 0 & 0 & 0 & 0 \end{bmatrix},
$$

$$
\boldsymbol{L}_y^{(4)} = \begin{bmatrix} 0 & \sqrt{2} & 0 & 0 & 0 & 0 & 0 & 0 & 0\\ -\sqrt{2} & 0 & \frac{\sqrt{7}}{2} & 0 & 0 & 0 & 0 & 0 & 0\\ 0 & -\frac{\sqrt{7}}{2} & 0 & \frac{3}{\sqrt{2}} & 0 & 0 & 0 & 0 & 0\\ 0 & 0 & -\frac{3}{\sqrt{2}} & 0 & 0 & 0 & 0 & 0 & 0\\ 0 & 0 & 0 & 0 & 0 & \sqrt{10} & 0 & 0 & 0\\ 0 & 0 & 0 & 0 & \sqrt{10} & 0 & -\frac{3}{\sqrt{2}} & 0 & 0\\ 0 & 0 & 0 & 0 & 0 & \frac{3}{\sqrt{2}} & 0 & -\frac{\sqrt{7}}{2} & 0\\ 0 & 0 & 0 & 0 & 0 & 0 & \frac{\sqrt{7}}{2} & 0 & -\sqrt{2}\\ 0 & 0 & 0 & 0 & 0 & 0 & 0 & \sqrt{2} & 0 \end{bmatrix},
$$

$$
\boldsymbol{R}_x^{(2)}(\frac{\pi}{2}) = \begin{bmatrix} 0 & 0 & 0 & -1 & 0\\ 0 & -1 & 0 & 0 & 0\\ 0 & 0 & -\frac{1}{2} & 0 & -\frac{\sqrt{3}}{2}\\ 1 & 0 & 0 & 0 & 0\\ 0 & 0 & -\frac{\sqrt{3}}{2} & 0 & \frac{1}{2} \end{bmatrix},
$$

$$
\boldsymbol{R}_z^{(2)}(\theta_i^z) = \begin{bmatrix} cos(2\theta_i^z) & 0 & 0 & 0 & sin(2\theta_i^z)\\ 0 & cos(\theta_i^z) & 0 & sin(\theta_i^z) & 0\\ 0 & 0 & 1 & 0 & 0\\ 0 & -sin(\theta_i^z) & 0 & cos(\theta_i^z) & 0\\ -sin(2\theta_i^z) & 0 & 0 & 0 & cos(2\theta_i^z) \end{bmatrix},
$$

*Corresponding author

Authors' addresses: Haikuan Zhu, hkzhu@wayne.edu, Wayne State University, USA; Hongbo Li, hm9026@wayne.edu, Wayne State University, USA; Hsueh-Ti Derek Liu, hsuehtil@gmail.com, Roblox & University of British Columbia, Canada; Wenping Wang, wenping@tamu.edu, Texas A&M University, USA; Jing Hua, jinghua@wayne.edu, Wayne State University, USA; Zichun Zhong, zichunzhong@wayne.edu, Department of Computer Science, Wayne State University, 5057 Woodward Ave., Suite 14109.2, Detroit, MI, USA, 48202.

$$
\boldsymbol{R}_z^{(4)}(\theta_i^z) = \begin{bmatrix}
cos(4\theta_i^z) & 0 & 0 & 0 & 0 & 0 & 0 & 0 & sin(4\theta_i^z) \\
0 & cos(3\theta_i^z) & 0 & 0 & 0 & 0 & 0 & sin(3\theta_i^z) & 0 \\
0 & 0 & cos(2\theta_i^z) & 0 & 0 & 0 & sin(2\theta_i^z) & 0 & 0 \\
0 & 0 & 0 & cos(\theta_i^z) & 0 & sin(\theta_i^z) & 0 & 0 & 0 \\
0 & 0 & 0 & 0 & 1 & 0 & 0 & 0 & 0 \\
0 & 0 & 0 & -sin(\theta_i^z) & 0 & cos(\theta_i^z) & 0 & 0 & 0 \\
0 & 0 & -sin(2\theta_i^z) & 0 & 0 & 0 & cos(2\theta_i^z) & 0 & 0 \\
0 & -sin(3\theta_i^z) & 0 & 0 & 0 & 0 & 0 & cos(3\theta_i^z) & 0 \\
-sin(4\theta_i^z) & 0 & 0 & 0 & 0 & 0 & 0 & 0 & cos(4\theta_i^z)
\end{bmatrix},
$$

$$
\boldsymbol{R}_x^{(4)}(\frac{\pi}{2}) = \begin{bmatrix}
0 & 0 & 0 & 0 & 0 & \frac{\sqrt{14}}{4} & 0 & -\frac{\sqrt{2}}{4} & 0 \\
0 & -\frac{3}{4} & 0 & \frac{\sqrt{7}}{4} & 0 & 0 & 0 & 0 & 0 \\
0 & 0 & 0 & 0 & 0 & \frac{\sqrt{2}}{4} & 0 & \frac{\sqrt{14}}{4} & 0 \\
0 & \frac{\sqrt{7}}{4} & 0 & \frac{3}{4} & 0 & 0 & 0 & 0 & 0 \\
0 & 0 & 0 & 0 & \frac{3}{8} & 0 & \frac{\sqrt{5}}{4} & 0 & \frac{\sqrt{35}}{8} \\
-\frac{\sqrt{14}}{4} & 0 & -\frac{\sqrt{2}}{4} & 0 & 0 & 0 & 0 & 0 & 0 \\
0 & 0 & 0 & 0 & \frac{\sqrt{5}}{4} & 0 & \frac{1}{2} & 0 & -\frac{\sqrt{7}}{4} \\
\frac{\sqrt{2}}{4} & 0 & -\frac{\sqrt{14}}{4} & 0 & 0 & 0 & 0 & 0 & 0 \\
0 & 0 & 0 & 0 & \frac{\sqrt{35}}{8} & 0 & -\frac{\sqrt{7}}{4} & 0 & \frac{1}{8}
\end{bmatrix}.
$$

1.2 Canonical Odeco Tensor

The full expression of the canonical odeco tensor $\hat{f}(\boldsymbol{\lambda}_i) \in \mathbb{R}^{15}$ is represented by bands 0, 2, and 4 of SH as follows:

$$
\begin{aligned}
\hat{f}(\boldsymbol{\lambda}_i) &= [\hat{f}^{(0)}(\boldsymbol{\lambda}_i), \hat{f}^{(2)}(\boldsymbol{\lambda}_i), \hat{f}^{(4)}(\boldsymbol{\lambda}_i)] \in \mathbb{R}^1 \times \mathbb{R}^5 \times \mathbb{R}^9, \\
\hat{f}^{(0)}(\boldsymbol{\lambda}_i) &= \frac{2}{5}\sqrt{\pi}(\lambda_i^x + \lambda_i^y + \lambda_i^z), \\
\hat{f}^{(2)}(\boldsymbol{\lambda}_i) &= [0, 0, \frac{4}{7}\sqrt{\frac{\pi}{5}}(2\lambda_i^z - (\lambda_i^x + \lambda_i^y)), 0, \frac{4}{7}\sqrt{\frac{3\pi}{5}}(\lambda_i^x - \lambda_i^y)], \\
\hat{f}^{(4)}(\boldsymbol{\lambda}_i) &= \begin{matrix} [0, 0, 0, 0, \frac{2}{35}\sqrt{\pi}(\lambda_i^x + \lambda_i^y + \frac{8}{3}\lambda_i^z), \\ 0, -\frac{4}{21}\sqrt{\frac{\pi}{5}}(\lambda_i^x - \lambda_i^y), 0, \frac{2}{3}\sqrt{\frac{\pi}{35}}(\lambda_i^x + \lambda_i^y)]. \end{matrix}
\end{aligned} \tag{1}
$$

1.3 Normal-Aligned Boundary Odeco Tensor

For a boundary vertex on the boundary $i \in \partial\Omega$ with normal direction $\vec{\boldsymbol{n}}_i \in \mathbb{R}^3$, we only allow rotation around the normal direction, which leaves us to only having θ_i^z as the only variable. Let (ρ, φ) represent the spherical coordinates of the direction $\vec{\boldsymbol{n}}_i$ such that $\vec{\boldsymbol{n}}_i = ||\vec{\boldsymbol{n}}_i||(sin\rho cos\varphi, sin\rho sin\varphi, cos\rho)$, the rotation matrix $\boldsymbol{R}_i \in \mathbb{R}^{15\times15}$ which brings the $\boldsymbol{z}$ axis to $\vec{\boldsymbol{n}}_i$ can be rewritten as $\boldsymbol{R}_i = e^{\varphi \mathrm{L}_z} e^{\rho \mathrm{L}_y} = e^{\varphi \mathrm{L}_z} e^{\frac{\pi}{2}\mathrm{L}_x} e^{\rho \mathrm{L}_z} e^{\frac{\pi}{2}\mathrm{L}_x}{}^T$. Thus, $\boldsymbol{R}_i$ is a constant 15×15 matrix determined by $\vec{\boldsymbol{n}}_i$. Combining with the rotation $e^{\theta_i^z \mathrm{L}_z}$ around the z-axis, we obtain

$$
f(\boldsymbol{\theta}_i, \boldsymbol{\lambda}_i) = \boldsymbol{R}_i e^{\theta_i^z \mathrm{L}_z} \boldsymbol{B}\boldsymbol{\lambda}_i, \quad \forall i \in \partial\Omega. \tag{2}
$$

1.4 Proof of Proposition 5.1

Let $f(\boldsymbol{\theta}_i, \boldsymbol{\lambda}_i), i \in \partial\Omega$ (for short f_i) be a normal-aligned odeco field on a smooth surface $\partial\Omega$ with the corresponding stretching ratios $(\lambda_i^x, \lambda_i^y, \lambda_i^z)$. We first set a local parametrization to a point i^* of the embedding via $\boldsymbol{v}_i : \mathbb{R}^{15} \to \mathbb{R}^3$, where $\boldsymbol{v}_i$ is the axis-angle rotation from f_{i^*} to f_i. Let axes $(\boldsymbol{\mu}, \boldsymbol{\nu})$ denote the principal curvature directions and become the local coordinates in the tangent plane. Without loss of generality, we rotate the normal of the point i^* to axis $\boldsymbol{z}$. However, the default axes $(\boldsymbol{x}, \boldsymbol{y})$ that define the canonical odeco tensor in the tangent plane are usually not $(\boldsymbol{\mu}, \boldsymbol{\nu})$. Therefore, we let ϕ denote the rotation angle that rotates the axes $(\boldsymbol{x}, \boldsymbol{y})$ to axes $(\boldsymbol{\mu}, \boldsymbol{\nu})$. Then, the odeco tensor f_i is expressed as:

$$
f_i = e^{\boldsymbol{v}_i \cdot [\boldsymbol{L}_x\ \boldsymbol{L}_y\ \boldsymbol{L}_z]} e^{\theta_i^z \boldsymbol{L}_z} e^{\phi \boldsymbol{L}_z} \hat{f},
$$

where θ_i^z is the free rotation angle around the normal. Note that, $v_i^z(\boldsymbol{\mu}, \boldsymbol{\nu}) = 0$ in terms of the way defined in Eq. (6) in our manuscript. Let $\bar{f} = e^{\phi \boldsymbol{L}_z}\hat{f}$ and $r(\boldsymbol{\mu}, \boldsymbol{\nu}) = [v_i^x(\boldsymbol{\mu}, \boldsymbol{\nu}), v_i^y(\boldsymbol{\mu}, \boldsymbol{\nu}), 0] + [0, 0, \theta_i^z]$ for shorthand, we obtain $f_i = e^{r \cdot [\boldsymbol{L}_x\ \boldsymbol{L}_y\ \boldsymbol{L}_z]}\bar{f}$. Following the gradient formula $\nabla f(\boldsymbol{\mu}, \boldsymbol{\nu})\big|_{i^*}$ derived from [Zhang et al. 2020] for the octahedral frames,

$$
\nabla f(\boldsymbol{\mu}, \boldsymbol{\nu})\big|_{i^*} = \begin{bmatrix} | & | & | \\ \boldsymbol{L}_x\bar{f} & \boldsymbol{L}_y\bar{f} & \boldsymbol{L}_z\bar{f} \\ | & | & | \end{bmatrix} \begin{bmatrix} | & | \\ \nabla_{\boldsymbol{\mu}} r & \nabla_{\boldsymbol{\nu}} r \\ | & | \end{bmatrix}_{i^*}.
$$

The squared norm $||\nabla f(\boldsymbol{\mu}, \boldsymbol{\nu})||_2^2$ at point i^* is

$$
\begin{aligned}
&||\nabla f(\boldsymbol{\mu}, \boldsymbol{\nu})||_2^2 = \\
&Tr(\begin{bmatrix} | & | \\ \nabla_{\boldsymbol{\mu}} r & \nabla_{\boldsymbol{\nu}} r \\ | & | \end{bmatrix}^T \begin{bmatrix} | & | & | \\ \boldsymbol{L}_x\bar{f}_{i^*} & \boldsymbol{L}_y\bar{f} & \boldsymbol{L}_z\bar{f} \\ | & | & | \end{bmatrix}^T \\
&\begin{bmatrix} | & | & | \\ \boldsymbol{L}_x\bar{f} & \boldsymbol{L}_y\bar{f} & \boldsymbol{L}_z\bar{f} \\ | & | & | \end{bmatrix} \begin{bmatrix} | & | \\ \nabla_{\boldsymbol{\mu}} r & \nabla_{\boldsymbol{\nu}} r \\ | & | \end{bmatrix}).
\end{aligned}
$$

According to the expression of Eq. (1) and $\bar{f} = e^{\phi \boldsymbol{L}_z}\hat{f}$, we get

$$
\begin{aligned}
\bar{f} = [&\frac{2}{5}\sqrt{\pi}(\lambda_1 + \lambda_2 + \lambda_3), sin(2\phi)\frac{4}{7}\sqrt{\frac{3\pi}{5}}(\lambda_1 - \lambda_2), 0, \\
&\frac{4}{7}\sqrt{\frac{\pi}{5}}(2\lambda_3 - (\lambda_1 + \lambda_2)), 0, cos(2\phi)\frac{4}{7}\sqrt{\frac{3\pi}{5}}(\lambda_1 - \lambda_2), \\
&sin(4\phi)\frac{2}{3}\sqrt{\frac{\pi}{35}}(\lambda_1 + \lambda_2), 0, -sin(2\phi)\frac{4}{21}\sqrt{\frac{\pi}{5}}(\lambda_1 - \lambda_2), 0, \\
&\frac{2}{35}\sqrt{\pi}(\lambda_1 + \lambda_2 + \frac{8}{3}\lambda_3), \\
&0, -cos(2\phi)\frac{4}{21}\sqrt{\frac{\pi}{5}}(\lambda_1 - \lambda_2), 0, cos(4\phi)\frac{2}{3}\sqrt{\frac{\pi}{35}}(\lambda_1 + \lambda_2)].
\end{aligned}
$$

It is easy to verify that $\bar{f}_{i^*}\boldsymbol{L}_m^T\boldsymbol{L}_n\bar{f}_{i^*} = 0$ for $\forall\phi \in \mathbb{R}$ $m, n \in \{\{y, z\}, \{x, z\}\}$. Given that $\boldsymbol{\mu}, \boldsymbol{\nu}$ are aligned with principal curvature directions, and K_{max}, K_{min} are principal curvatures at point i^*, we have $\frac{\partial v_i^x}{\partial \boldsymbol{\mu}} = 0$, $\frac{\partial v_i^x}{\partial \boldsymbol{\nu}} = K_{max}$, $\frac{\partial v_i^y}{\partial \boldsymbol{\mu}} = K_{min}$, $\frac{\partial v_i^y}{\partial \boldsymbol{\nu}} = 0$. Therefore, we obtain

$$
\begin{aligned}
&||\nabla f(\boldsymbol{\mu}, \boldsymbol{\nu})||_2^2 = \\
&Tr(\begin{bmatrix} \frac{\partial v_i^x}{\partial \boldsymbol{\mu}} & \frac{\partial v_i^x}{\partial \boldsymbol{\nu}} \\ \frac{\partial v_i^y}{\partial \boldsymbol{\mu}} & \frac{\partial v_i^y}{\partial \boldsymbol{\nu}} \\ \frac{\partial \theta_i^z}{\partial \boldsymbol{\mu}} & \frac{\partial \theta_i^z}{\partial \boldsymbol{\nu}} \end{bmatrix}^T \begin{bmatrix} \bar{f}\boldsymbol{L}_x^T\boldsymbol{L}_x\bar{f} & | & 0 \\ | & \bar{f}\boldsymbol{L}_y^T\boldsymbol{L}_y\bar{f} & 0 \\ 0 & 0 & \bar{f}\boldsymbol{L}_z^T\boldsymbol{L}_z\bar{f} \end{bmatrix} \begin{bmatrix} \frac{\partial v_i^x}{\partial \boldsymbol{\mu}} & \frac{\partial v_i^x}{\partial \boldsymbol{\nu}} \\ \frac{\partial v_i^y}{\partial \boldsymbol{\mu}} & \frac{\partial v_i^y}{\partial \boldsymbol{\nu}} \\ \frac{\partial \theta_i^z}{\partial \boldsymbol{\mu}} & \frac{\partial \theta_i^z}{\partial \boldsymbol{\nu}} \end{bmatrix}) \\
&= (\bar{f}\boldsymbol{L}_x^T\boldsymbol{L}_x\bar{f})K_{max}^2 + (\bar{f}\boldsymbol{L}_y^T\boldsymbol{L}_y\bar{f})K_{min}^2 + (\bar{f}\boldsymbol{L}_z^T\boldsymbol{L}_z\bar{f})((\frac{\partial \theta_i^z}{\partial \boldsymbol{\mu}})^2 + (\frac{\partial \theta_i^z}{\partial \boldsymbol{\nu}})^2).
\end{aligned}
$$

Then, we derive

$$\bar{f}\boldsymbol{L}_x^T\boldsymbol{L}_x\bar{f} = cos^2(\phi)g_1(\boldsymbol{\lambda_i}) + sin^2(\phi)g_2(\boldsymbol{\lambda_i}),$$
$$\bar{f}\boldsymbol{L}_y^T\boldsymbol{L}_y\bar{f} = sin^2(\phi)g_1(\boldsymbol{\lambda_i}) + cos^2(\phi)g_2(\boldsymbol{\lambda_i}),$$
$$\bar{f}\boldsymbol{L}_z^T\boldsymbol{L}_z\bar{f} = g_3(\boldsymbol{\lambda_i}),$$

where $g_i(\boldsymbol{\lambda_i}) = \frac{64\pi}{315}(4(\lambda_i^m - \lambda_i^n)^2 + (\lambda_i^m + \lambda_i^n)^2)$, $m, n \in \{\{y,z\},\{x,z\},\{x,y\}\}$ for $k = 1,2,3$. Finally, substituting ω to $(\frac{\partial\theta_i^z}{\partial\boldsymbol{\mu}})^2 + (\frac{\partial\theta_i^z}{\partial\boldsymbol{\nu}})^2$, the square norm $||\nabla f(\boldsymbol{\mu},\boldsymbol{\nu})||_2^2$ is re-expressed as

$$||\nabla f(\boldsymbol{\mu},\boldsymbol{\nu})||_2^2 =$$
$$(cos^2(\phi)g_1(\boldsymbol{\lambda_i}) + sin^2(\phi)g_2(\boldsymbol{\lambda_i}))K_{max}^2 +$$
$$(sin^2(\phi)g_1(\boldsymbol{\lambda_i}) + cos^2(\phi)g_2(\boldsymbol{\lambda_i}))K_{min}^2 +$$
$$g_3(\boldsymbol{\lambda_i})\omega.$$

The smoothness energy $||\nabla f||_2^2$ is divided into the extrinsic curvature-aligned term $(cos^2(\phi)g_1(\boldsymbol{\lambda_i}) + sin^2(\phi)g_2(\boldsymbol{\lambda_i}))K_{max}^2 + (sin^2(\phi)g_1(\boldsymbol{\lambda_i}) + cos^2(\phi)g_2(\boldsymbol{\lambda_i}))K_{min}^2$ and the intrinsic tangential twisting term $g_3(\boldsymbol{\lambda_i})\omega$.

1.5 Proof of Proposition 5.2

We denote

$$a(\phi,\boldsymbol{\lambda_i}) = cos^2(\phi)g_1(\boldsymbol{\lambda_i}) + sin^2(\phi)g_2(\boldsymbol{\lambda_i}),$$
$$b(\phi,\boldsymbol{\lambda_i}) = sin^2(\phi)g_1(\boldsymbol{\lambda_i}) + cos^2(\phi)g_2(\boldsymbol{\lambda_i}).$$

Thus, the curvature-aligned term is re-express as $a(\phi,\boldsymbol{\lambda_i})K_{max}^2 + b(\phi,\boldsymbol{\lambda_i})K_{min}^2$ for short, where

$$a(\phi,\boldsymbol{\lambda_i}) + b(\phi,\boldsymbol{\lambda_i}) = g_1(\boldsymbol{\lambda_i}) + g_2(\boldsymbol{\lambda_i}).$$

Clearly,

$$g_2(\boldsymbol{\lambda_i}) - g_1(\boldsymbol{\lambda_i}) = C(\lambda_i^x - \lambda_i^y)(\frac{5}{6}(\lambda_i^x + \lambda_i^y) - \lambda_i^z).$$

If $\lambda_i^x \neq \lambda_i^y$ and $\lambda_i^z \neq \frac{5}{6}(\lambda_i^x + \lambda_i^y)$, we have $g_2(\boldsymbol{\lambda_i}) \neq g_1(\boldsymbol{\lambda_i})$, as well as $a(\phi,\boldsymbol{\lambda_i}) \neq b(\phi,\boldsymbol{\lambda_i})$. Given that K_{min} is the minimum principal curvature, therefore, minimizing $a(\phi,\boldsymbol{\lambda_i})K_{max}^2 + b(\phi,\boldsymbol{\lambda_i})K_{min}^2$ is equivalent to minimize $a(\phi,\boldsymbol{\lambda_i})$. It follows that, $a(\phi,\boldsymbol{\lambda_i})$ will be minimized if $sin^2(\phi)$ goes to 0 or 1, which reveals that the odeco tensor lobes need to be aligned with principal curvature directions.

Moreover, when $\lambda_i^z < \frac{5}{6}(\lambda_i^x + \lambda_i^y)$, here we assume that $\lambda_i^x > \lambda_i^y$, we have $g_2(\boldsymbol{\lambda_i}) > g_1(\boldsymbol{\lambda_i})$. When $g_2(\boldsymbol{\lambda_i}) > g_1(\boldsymbol{\lambda_i})$ and $sin^2(\phi)$ goes to 0, $a(\phi,\boldsymbol{\lambda_i})$ will be minimized. $\lambda_i^x > \lambda_i^y$ and $sin^2(\phi) = 0$ indicate exact alignment between the lobe with a larger stretching ratio and the minimum principal curvature direction. Similarly, the same result will be obtained when $\lambda_i^x < \lambda_i^y$.

1.6 Proof of Proposition 5.3

Let f_1, f_2 represent two normal-aligned odeco tensors whose tangent planes are intersected at the feature edges. We let f_1, f_2 have the same stretching ratios due to the continuity in a local area. Let φ_1, φ_2 denote the deviation angles between the lobe with the larger stretching ratio on the tangent plane and the direction of the feature edge. Without loss of generality, we let $\hat{f}$ be the canonical odeco tensor, $f_1 = e^{\varphi_1\boldsymbol{L}_z}\hat{f}$ and $f_2 = e^{\delta\boldsymbol{L}_y}e^{\varphi_2\boldsymbol{L}_z}\hat{f}$, where δ is the dihedral angle between two tangent planes. The difference between these two odeco tensors is

$$D(\varphi_1,\varphi_2) = ||f_1 - f_2||_2^2$$
$$= ||e^{\varphi_1\boldsymbol{L}_z}\hat{f} - e^{\delta\boldsymbol{L}_y}e^{\varphi_2\boldsymbol{L}_z}\hat{f}||_2^2$$
$$= (e^{\varphi_1\boldsymbol{L}_z}\hat{f} - e^{\delta\boldsymbol{L}_y}e^{\varphi_2\boldsymbol{L}_z}\hat{f})^T(e^{\varphi_1\boldsymbol{L}_z}\hat{f} - e^{\delta\boldsymbol{L}_y}e^{\varphi_2\boldsymbol{L}_z}\hat{f}).$$

We assume $D(\varphi_1,\varphi_2)$ is minimized by $\varphi_1 = \varphi_2 = 0 \pm n\pi, n \in \mathbb{Z}$, since D is only composed of lots of terms of $cos(2\varphi_1), cos(2\varphi_2)$, we only need to prove $D(0,0)$ is the minimum for all $\lambda_i^x \geq \lambda_i^y, \lambda_i^z, \delta$, i.e., the solution (φ_1,φ_2) of $D(\varphi_1,\varphi_2) - D(0,0) < 0$ is empty. To avoid matrix exponential computations, we provide the related rotation matrices in Section 1.1. By denoting $e^{\varphi_1\boldsymbol{L}_z}$, $e^{\varphi_1\boldsymbol{L}_z}$, $e^{\delta\boldsymbol{L}_y}$ as $Rz(\varphi_1)$, $Rz(\varphi_2)$, $Ry(\alpha)$, respectively. We have

$$D(\varphi_1,\varphi_2) - D(0,0) =$$
$$(Rz(\varphi_1)\hat{f} - Ry(\alpha)Rz(\varphi_2)\hat{f})^T(Rz(\varphi_1)\hat{f} - Ry(\alpha)Rz(\varphi_2)\hat{f})$$
$$- (\hat{f} - Ry(\alpha)\hat{f})^T(\hat{f} - Ry(\alpha)\hat{f}).$$

Our proof is assisted by the MATLAB Symbolic computations. For any given $\lambda_i^x \geq \lambda_i^y, \lambda_i^z, \delta$, the solution of $D(\varphi_1,\varphi_2) - D(0,0) < 0$ remains empty. Besides that, Fig. 4 in our manuscript demonstrates the function of $D(\varphi_1,\varphi_2)$ for a specific case.

1.7 A Simple Demo for Proposition 5.2

In Fig. S1, we validate the theoretical analysis of Proposition 5.2 by a simple demo. Here, we specify three different stretching ratios for the entire domain. For each $\boldsymbol{\lambda}_i$, we have $5:1:1$ ($\lambda_i^z < \frac{5}{6}(\lambda_i^x + \lambda_i^y)$) in Fig. S1 (a), $5:1:8$ ($\lambda_i^z > \frac{5}{6}(\lambda_i^x + \lambda_i^y)$) in Fig. S1 (b), and $5:1:5$ ($\lambda_i^z = \frac{5}{6}(\lambda_i^x + \lambda_i^y)$) in Fig. S1 (c). Compared with the distribution of local minima of random trials, case (c) is highly non-convex. Both (a) and (b) only need a single trial to achieve global minimum for the Torus model. However, it is hard to find the global minimum for (c) since the curvature guidance disappears according to Proposition 5.2.

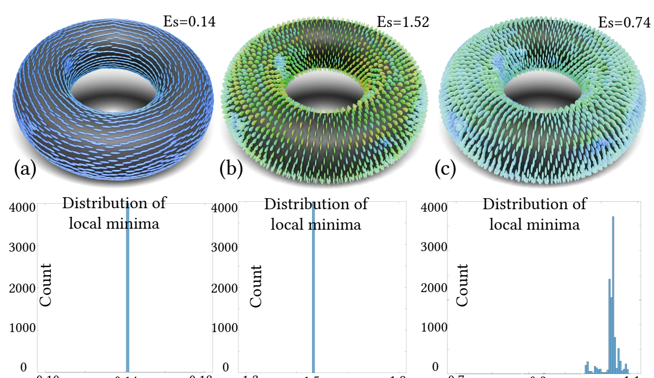

Fig. S1. Evaluation on the setting of stretching ratios $\boldsymbol{\lambda}_i^{In}$. Top: (a, b, c) are optimal solutions with different specified stretching ratios. Bottom: the distributions of 4,000 local minima of random trials for each case. (a,b) only need one trial to get the global minimum; however, (c) takes lots of trials to find the global minimum.

REFERENCES

Paul Zhang, Josh Vekhter, Edward Chien, David Bommes, Etienne Vouga, and Justin Solomon. 2020. Octahedral frames for feature-aligned cross fields. *ACM Transactions on Graphics* 39, 3 (2020), 1–13.

Received XXXXX; revised XXXXXX; accepted XXXXXX